(15) Rehage, G.; Goldbach, G. *Ber. Bunsenges. Phys. Chem.* **1966**, *70*, 1144.
(16) Goldbach, G.; Rehage, G. *J. Polym. Sci., Part C* **1967**, *16*, 2289.
(17) Kovacs, A. J. *J. Polym. Sci.* **1958**, *30*, 131.
(18) Hozumi, S.; Wakabayashi, T.; Sugihara, S. *Polym. J.* **1970**, *1*, 632.
(19) Uchidoi, M.; Adachi, K.; Ishida, Y. *Polym. J.* **1978**, *10*, 161.
(20) Adachi, K.; Kotaka, T. *Polym. J.* **1982**, *14*, 959.
(21) Kogowski, G. J.; Filisko, F. E. *Macromolecules*, in press.
(22) Kogowski, G. J.; Robertson, R. E.; Filisko, F. E., to be published.
(23) Oels, H. J.; Rehage, G. *Macromolecules* **1977**, *10*, 1036.
(24) Rehage, G. *Ber. Bunsenges. Phys. Chem.* **1970**, *74*, 796.
(25) Fillers, R. W.; Tschoegl, N. W. *Trans. Soc. Rheol.* **1977**, *21*, 51.
(26) Moonan, W. K.; Tschoegl, N. W. *Macromolecules* **1983**, *16*, 55.
(27) Cogswell, F. N.; McGowan, J. C. *Br. Polym. J.* **1972**, *4*, 183.
(28) Plazek, D. J. *J. Phys. Chem.* **1965**, *69*, 3480.
(29) Plazek, D. J.; O'Rourke, V. M. *J. Polym. Sci., Part A-2* **1971**, *9*, 209.
(30) Plazek, D. J. *Polym. J.* **1980**, *12*, 43.

Theoretical Study of the Influence of the Molecular Weight on the Maximum Tensile Strength of Polymer Fibers

Yves Termonia,* Paul Meakin, and Paul Smith

Central Research and Development Department, Experimental Station, E. I. du Pont de Nemours and Company, Inc., Wilmington, Delaware 19898. *Received March 9, 1985*

ABSTRACT: A stochastic Monte Carlo approach, based on the kinetic theory of fracture, has been used to study the axial maximum tensile strength of polymer fibers. The approach is entirely microscopic and the inhomogeneous distribution of the external stress among atomic bonds near the chain ends is explicitly taken into account. Both primary and secondary bonds are assumed to break during fracture of the polymer fiber. The approach has been applied to perfectly oriented and ordered polyethylene fibers, for which approximate values of the model's parameters were obtained from experiment. Stress–strain curves have been calculated for several fibers of various (monodisperse) molecular weights and predictions for the tensile strength have been compared to experimental values.

1. Introduction

Values of the maximum tensile modulus have been measured or calculated for many polymers[1] and have proven to be very useful in setting goals for polymer materials research.[2-4] The maximum tensile strength of polymers is a less satisfying issue. Some authors, with widely different results, have addressed the theoretical ultimate breaking stress of single chains.[5-7] Such treatments, however, are only of value for hypothetical specimens comprising infinitely long chain molecules and are not necessarily relevant for finite molecular weights. Experimental tensile strength data, obtained for drawn fibers, have been extrapolated to infinitely small fiber diameter[8] and this procedure has led sometimes to agreement with some of the above-mentioned values for the breaking stress of a single chain. Some attempts have been made to describe the development of tensile strength with draw ratio[9,10], and purely empirical extrapolations of the tensile strength to the theoretical modulus have also been reported.[11,12] Despite various theoretical and some empirical efforts, no relation for relatively simple issues such as the effect of the molecular weight on the maximum tensile strength has appeared in the polymer literature, other than Flory's expression[13] for the tensile strength of cross-linked isotropic rubbers. All in all, the maximum tensile strength of polymeric materials of finite molecular weight and the relation to the ultimate breaking stress of infinitely long chains remains an obscure, ill-understood topic.

A theoretical study of the tensile strength of polymer fibers is an extremely complex problem. Many structural parameters, such as amorphous defects, trapped entanglements, chain ends, misalignment, etc., need to be considered. In fact, a detailed knowledge of the fiber structure is required on a molecular level. But, even in the presence of such information, a theoretical treatment of the tensile properties remains an enormous task. For that reason, all previous theories have made many simplifying assumptions with regard to the structure and the failure mechanism. For example, classical continuum mechanics, e.g., Griffith-type approaches,[14] fail to take into account the inhomogeneous nature of the structures of interest. Kinetic theories of fracture commonly focus on only one mode of failure, i.e., merely primary bond breakage,[15,16] or pure slippage,[17,18] while both mechanisms are known to operate during fracture of polymer fibers.[19] Other kinetic theories[20] ignore the important contributions of the intermolecular interactions altogether.

Due to the complexity of a general theoretical treatment of the strength of polymer fibers, the present study is restricted to the case of ideal fibers made of a perfectly ordered array of fully extended macromolecules, with no defects other than chain ends resulting from finite molecular weight. As such, the study deals with the maximum axial tensile strength, which is of obvious interest, much like the knowledge of the theoretical modulus has proven to be. The present approach, which is based on the kinetic theory of fracture, is entirely microscopic and the inhomogeneous distribution of the external stress among atomic bonds near the chain ends is explicitly taken into account. The bonds are viewed as coupled oscillators in a state of constant thermal vibration. The basic events are controlled by thermally activated bond breakage and the accumulation of those events leads to crack formation and, ultimately, to the breakdown of the fiber. The bond breakages are simulated by a Monte Carlo process on a three-dimensional array of nodes, representing the elementary repetition unit of a polymer. These nodes are joined in the x and z directions by weak secondary bonds, e.g., hydrogen or van der Waals forces, whereas in the y direction, stronger bonds account for the primary (C–C) forces. Our model thus resembles that of Dobrodumov and El'yashevitch[21] except for the fact that, in the latter, it was assumed that only primary bonds can break. Here, in contrast, we allow fiber fracture to proceed by the breaking

0024-9297/85/2218-2246$01.50/0

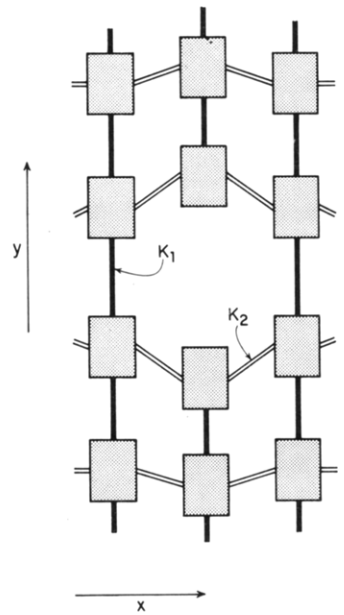

Figure 1. Two-dimensional representation of the array of nodes and of bonds. K_1 and K_2 are the elastic constants for the primary and for the secondary bonds, respectively.

of both primary and secondary bonds.

This approach has been applied to perfectly oriented and ordered polyethylene for which approximate values of the model's parameters can be obtained from experiment. With the help of our zero-parameter model, we have calculated the stress–strain curves for several fibers of various (monodisperse) molecular weights, and predictions for the tensile strength have been compared to extrapolated experimental values.

2. Stochastic Model

In the kinetic theory of fracture, a bond in the absence of external mechanical forces breaks whenever it becomes excited beyond a certain level, U, the activation energy of the bond. For molecular chains in the process of being strained, there is overriding experimental evidence from infrared studies[22] that the activation energy barrier is linearly decreased by the local stress. Thus, in the presence of stress, the rate of breakage of a bond i is given by

$$\upsilon_i = \tau \exp[(-U_i + \beta_i\sigma_i)/kT] \tag{1}$$

where τ is the thermal vibration frequency, T is the (absolute) temperature, β_i is an activation volume whose linear dimension is of the order of the bond length, and σ_i is the local stress

$$\sigma_i = K_i\epsilon_i \tag{2}$$

Here, K_i and ϵ_i are the elastic constant and the local strain, respectively. Note that, strictly speaking, the bilinear form $\beta\sigma$ should be a scalar. However, this is of little concern to the simulation, for which real numbers are substituted for the products $\beta\sigma$.

The above kinetic model has been simulated on a three-dimensional (x,y,z) array of up to $6 \times 6 \times 1000$ nodes representing the elementary repetition units of the polymer chains. (For very long chains, each node is made to correspond to more than one repetition unit; see section 4.) The number of chains per cross-sectional area thus amounts up to 36. The nodes are joined in the x and z directions by secondary bonds, e.g., hydrogen or van der Waals forces, having an elastic constant K_2. Only nearest-neighbor interactions are considerded. In the y direction, stronger forces with elastic constant K_1 account for the primary (C–C) bonds. A two-dimensional representation of the array of nodes is given in Figure 1. In the absence of stress, the nodes are in contact with each other along the y axis so that the length of a node actually represents the length of an unstrained C–C bond. We assume these nodes to be incompressible. For simplicity, we also assume that the displacements of the network nodes along the coordinate axes are mutually independent[21] and we focus on the displacement along the y axis, along which the fiber is strained. Thus, the strain values ϵ (see eq 2) are for elongations along the y axis and they represent either an axial tensile strain (for primary bonds) or a shear strain (for secondary bonds). These strain values are in percent of the length of a node along the y axis.

The simulation is started from an unstrained array in which all the bonds are unbroken, except for few broken C–C bonds along the y axis, which account for the finite molecular weight of the polymer chains. The unbroken bonds are visited at random by a Monte Carlo lottery that breaks a bond according to a probability

$$P_i = \upsilon_i/\upsilon_{max} \tag{3}$$

where υ_{max} is the rate of breakage of the most strained bond in the array. After each visit of a bond, the "time" t is incremented by $1/[\upsilon_{max}n(t)]$, where $n(t)$ is the total number of intact bonds at time t. After a small time interval δt has elapsed, the bond-breaking process is stopped. Of course, δt must be chosen much smaller than the shortest time for a single bond breaking; i.e., $\delta t \ll 1/\upsilon_{max}$. This has led us to take $\delta t = 0.01$ s, which was found to be sufficiently small to ensure that our results are δt independent. The sample is then strained along the y axis by a small constant amount and the network is relaxed to its minimum-energy configuration, using the method described in section 3. This leads to displacements of the nodes along the y axis. After that step, secondary bonds are allowed to re-form between nodes coming in perfect register to each other, to within a small error δy.[23] The alternation of breaking and relaxation steps for the secondary bonds should be equivalent to the use of a sinusoidal potential for the shear forces. Primary covalent bonds, however, are assumed not to re-form.[24] The system is then relaxed again and the axial stress at one end of the "fiber" is calculated. The Monte Carlo process of bond breaking is then restarted for another time interval δt. And so on and so forth until the sample breaks. This procedure, performed at a constant strain rate, yields a stress–strain curve, the maximum of which is referred to as the maximum tensile strength of the fiber for a given molecular weight under specified "test conditions".

Results of a simulation for a two-dimensional x–y array are illustrated in Figure 2 for a low (case a) and for a high (case b) elongation, respectively. Cylindrical boundary conditions along the x axis were imposed. Note the development of a large fracture focus in Figure 2b, which appears as a result of an acceleration of its growth due to the high concentration of stresses at its boundary.

3. Relaxation Method

The relaxation of the system to its minimum-energy configuration is realized in a sequence of steps. At each step, a node i is visited and its y ordinate is adjusted so as to to bring to zero the net residual stress (r)

$$r_i = \sum_{\text{bonds } j} \psi_j K_j \epsilon_j + \sum_{\text{nodes } i'} \xi_{i'} r_{i'} \tag{4}$$

acting on that node. The first term on the right-hand side of eq 4 is due to the elastic stress acting on the bonds j originating from node i, with $\psi_j = 1$ or $\psi_j = 0$ depending

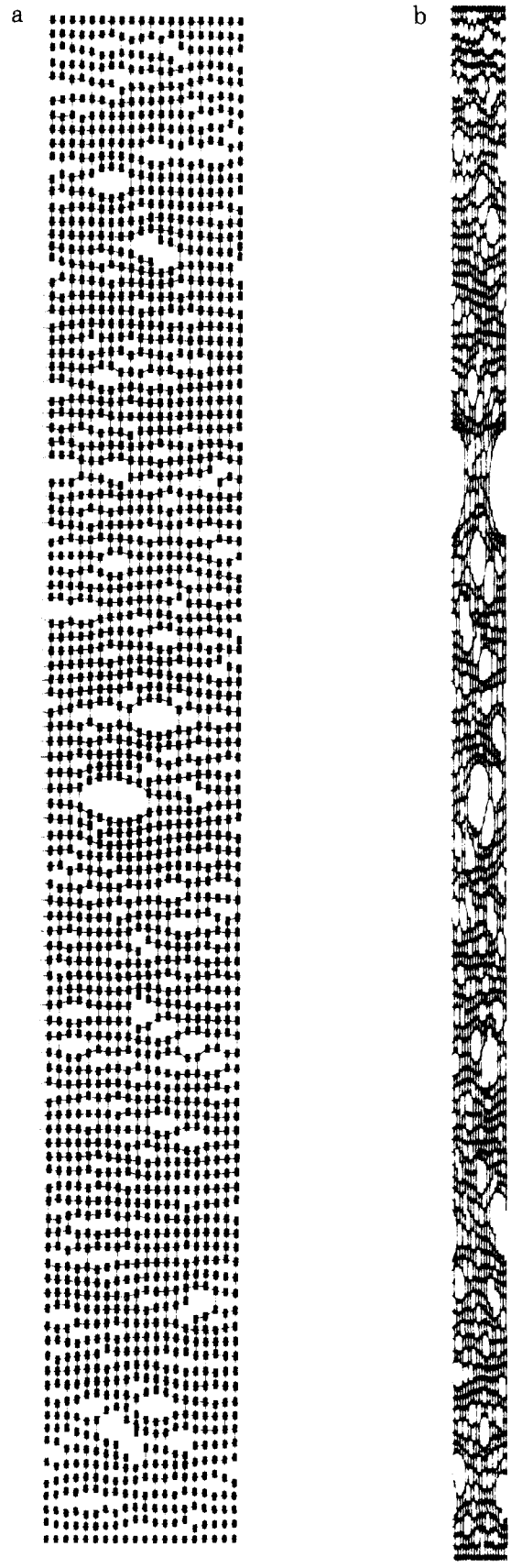

Figure 2. Results of the simulation for a two-dimensional array of 20 × 100 nodes: case a, 150% strain; case b, 300% strain. The probabilities for breaking primary and secondary bonds in these highly stretched samples were chosen equal to $\exp(\epsilon^2)$ for simplicity. Cylindrical boundary conditions along the x axis were imposed.

on whether bond j is intact or broken. Also, $K_j = K_1$ and $K_j = K_2$ for a primary and for a secondary bond, respectively. ϵ_j is the local strain measured by the difference in the y coordinates of the two ends of the bond. That latter value is in percent of the length of a node. The second term on the right-hand side of eq 4 accounts for the external forces acting on node i when in contact with any of its two neighbors i' along the y axis. Indeed, we recall our assumption that the nodes are incompressible, i.e., that the length of a C–C bond cannot be decreased below its equilibrium value in the absence of stress. Of course, $\xi_{i'} = 1$ or $\xi_{i'} = 0$, depending on whether contact with node i' is made or not.

It is important to note that bringing to zero the residual stress r_i for a node often results in an automatic increase of (the absolute value of) the residuals for the neighboring nodes. Therefore, the liquidation of all the residuals in the array is a very computer time-consuming process. For that reason, the liquidation of the residuals has been performed by using two well-known computational devices,[25] which considerably speed up the convergence of the calculations. The first device, known as overrelaxation, consists of not just reducing to zero the residual r_i for a node but, instead, deliberately going further to give to r_i a sign that is opposite that of the residuals for the neighboring nodes. The second, and more important, device is known as block relaxation and consists of adjusting the ordinates of more than one node at a time. Relaxation of the system using the above two devices was considered to be completed when the largest residual stress for a node fell below a few percent of the average stress for a bond.

4. Results: Application to Polyethylene

The stochastic model described in sections 2 and 3 has been applied to a hypothetical structure of perfectly oriented and ordered polyethylene, for which approximate values of the parameters in eq 1 and 2 are available. For secondary bonds the shear modulus $K_2 = 3$ GPa[26] and we took $U = 0.65$ kcal/mol with $\beta = (2.5\ \text{Å})^3$; for primary bonds the axial modulus $K_1 = 300$ GPa,[26] $U = 25$ kcal/mol,[22] and we chose $\beta = (1.54\ \text{Å})^3$. The atomic vibration frequency τ was chosen equal to 10^{11} s^{-1} [22] at $T = 300$ K. Thus, there are no free parameters in the model. Admittedly, the literature reveals a relatively wide scatter in the values for these parameters. Our value for U of the primary bonds of polyethylene is low compared to dissociation energies of ~80 kcal/mol commonly attributed to the C–C bond. However, the choice $U = 25$ kcal/mol is motivated by the fact that the latter value, reported in ref 22, has been obtained from a thermal fluctuation approach to fracture, like the present.[27] Note also that activation volumes are rather difficult to measure experimentally and the selection $U = 25$ kcal/mol is further consistent with taking the lowest value, $\beta = (1.54\ \text{Å})^3$, for the activation volume of the C–C bond. That uncertainty in the experimental data has led us to investigate the sensitivity of the calculated tensile strength to the values chosen for the parameters. It was found that the maximum stress is not appreciably affected by an increase or a decrease of τ by a factor of 10. Neither does it change significantly when taking $U = 80$ kcal/mol together with $\beta = (2.75\ \text{Å})^3$ for primary bonds. A choice $U = 80$ kcal/mol with $\beta = (1.54\ \text{Å})^3$ leads to notably higher values of the strength only at $M > 2 \times 10^5$ (see Discussion). Finally, it should be noted that, for reasons of computational time and memory, an important structural assumption was made in the application of our model to polyethylene. Namely, in the model, the coordination number in the x–z plane is 4, whereas the central chain in the crystalline orthorhombic polyethylene

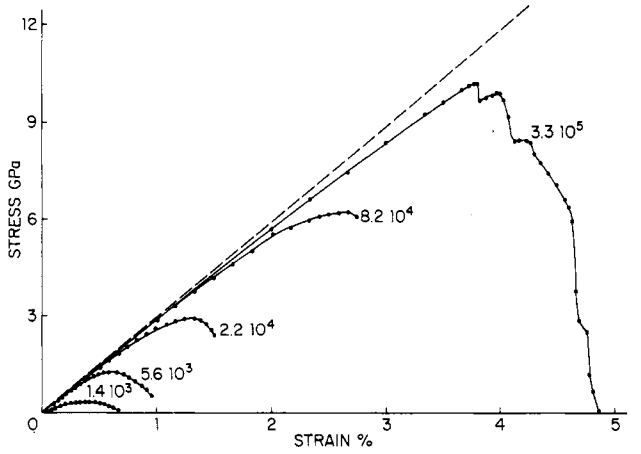

Figure 3. Stress–strain curves calculated for several polyethylene fibers of various (monodisperse) molecular weights. The strain rate is 100%/min. Three-dimensional simple cubic arrays of up to 6 × 6 × 1000 nodes were used in the simulations. Cylindrical boundary conditions along the x axis were imposed. Curves for $M = 2.2 \times 10^4$ and $M = 8.2 \times 10^4$ have not beed calculated in their entirety, due to a lack of computer time. The dashed line indicates a slope equal to the theoretical modulus (=300GPa).

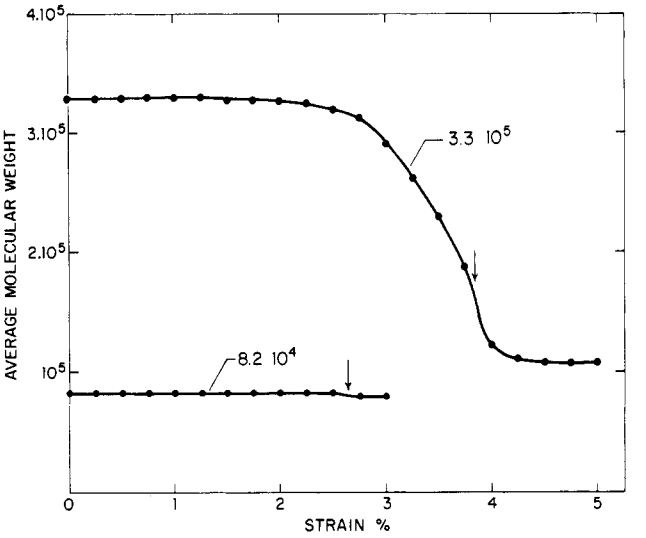

Figure 4. Dependence of the average molecular weight on the strain for two of the experiments reported in Figure 3. The arrow indicates the maximum in the corresponding stress–strain curve (see Figure 3).

unit cell has four chains at a distance of 4.4 Å and two neighbors at 4.8 Å. It is therefore obvious that the results presented in this section should not be interpreted too quantitatively. Rather, they should be taken as expected trends.

A set of stress–strain curves was calculated for various (monodisperse) molecular weights ranging from 3×10^2 to 3×10^5. The upper limit was set by the availability of computer time and memory. At high molecular weights, the following renormalization scheme has been adopted. Nodes were made to correspond to $m > 1$ methyl groups each, and the m secondary bonds linking two neighboring nodes were broken in groups of 25 units at a rate given by eq 1 and 2, with $U = 25 \times 0.65$ kcal/mol, $K_2 = 25 \times 3$ GPa, and τ and β having the same value as for a single secondary bond.[28] (For $m < 25$, the secondary bonds were broken in groups of five units.) Three-dimensional (simple cubic) arrays of up to 6 × 6 × 1000 nodes, with cylindrical boundary conditions along the x axis, were used in the simulations. The "test samples" comprised 36 chains per cross-section and had a length of ~16 chains. Increasing the number of chains per cross-section to 64 at the expense of a reduction of the length did not affect the results of the calculations, nor did the opposite operation. These observations indicate that our system is sufficiently homogeneous for the qualitative purposes of this work.

The stress–strain curves obtained for several fibers of various (monodisperse) molecular weights at a strain rate of 100%/min are depicted in Figure 3. Curves at intermediate molecular weights have not been represented in their entirety, due a lack of computer time. The stress values are those for the average stress in the primary bonds located at one end of the fiber. At low molecular weights ($M < 8 \times 10^4$), the results show that intermolecular slippage, involving rupture of secondary bonds, occurs in preference to molecular fracture (i.e., primary bond breakage). Under such circumstances, plastic deformation by flow is observed and the curves exhibit a bell shape with a very slow decrease of the stress toward the breaking point (see Figure 3, $M = 5.6 \times 10^3$). At high molecular weights ($M > 8 \times 10^4$), we observe primary as well as secondary bond rupture and, as a result (see Figure 3, $M = 3.3 \times 10^5$), the fracture of the sample seems more of a brittle nature. This observation is more clearly depicted in Figure 4. In this graph, the changes of the average molecular weight, monitored during the strain "experiment", are plotted for two different cases ($M_{initial} = 8.2 \times 10^4$ and 3.3×10^5). Interestingly enough, the high molecular weight "specimen" appears to fail first in a brittle manner and, second, in a creep-like mode due to the reduced average molecular weight. This will be commented upon in section 5.

Inspection of the stress–strain curves in Figure 3 also shows that the initial modulus of the sample is only weakly dependent on the molecular weight and it virtually can be considered to be constant (=300 GPa) for values of $M > 10^4$. The strain at failure (Figure 3) is of the order of a few percent, corresponding to a time to fracture of 1–3 s, in excellent agreement with experimental results on highly oriented fibers[1-4,8-12] tested under similar conditions.

Further study shows that the stress concentration factor, i.e., the ratio of the local stress and the mean stress, can attain values as large as 10, in good accordance with experimental findings.[22] Figure 5 shows the stress distribution for a high molecular weight fiber ($M = 3.3 \times 10^5$) slightly before ($t = 2$ s) and at ($t = 2.4$ s) the maximum in the stress–strain curve (see Figure 3). The stresses are in units of the average stress in the type of bond being considered. Inspection of the figure shows an important widening in the distribution function as the breaking point is approached. This again stresses the importance of a detailed microscopic approach to fracture, like the present, in which the inhomogeneous distribution of the external stress among atomic bonds is explicitly taken into account. Note, finally, the similarity of the curves in Figure 5 to experimental data reported in ref 22 for fracture of polypropylene.

Figure 6 shows the calculated dependence (on a log–log scale) of the tensile strength (maximum of the curves in Figure 3) on the molecular weight. Symbols indicate different values used in the simulation for the number m of methyl groups per node. The figure reveals that the results for the maximum strength at a given molecular weight are rather insensitive to the value chosen for m (provided that the number of nodes per chain is renormalized accordingly). This leads to confidence in the validity of our (admittedly crude) renormalization procedure. The tenacity/molecular weight curve in Figure 6 displays no simple power law dependency. Rather, the slope of the curve changes continuously. The lack of a simple relation

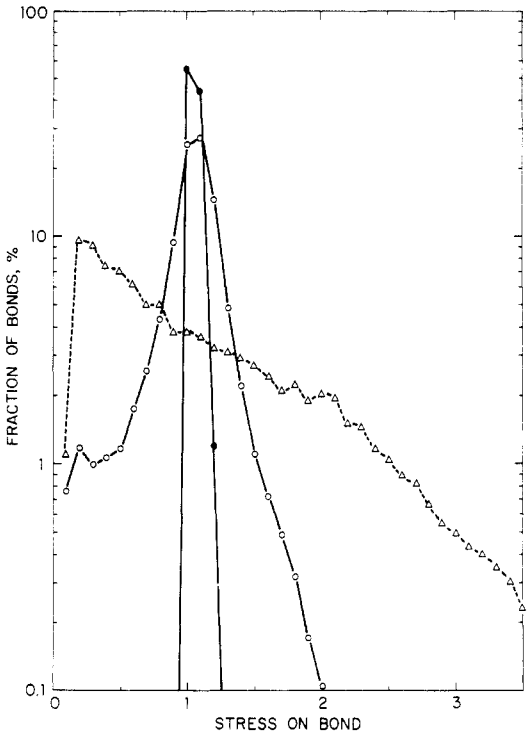

Figure 5. Stress distribution for monodisperse polyethylene with $M = 3.3 \times 10^5$ slightly below ($t = 2$ s (●)) and at ($t = 2.4$ s (○, △)) the maximum in the stress–strain curve (see Figure 3). The continuous curve is for primary bonds; the dashed curve is for secondary bonds. The stress in a bond is in units of the average stress in that bond. For clarity, the stress distribution for the secondary forces at $t = 2$ s has not been represented, since it is similar to that observed at $t = 2.4$ s.

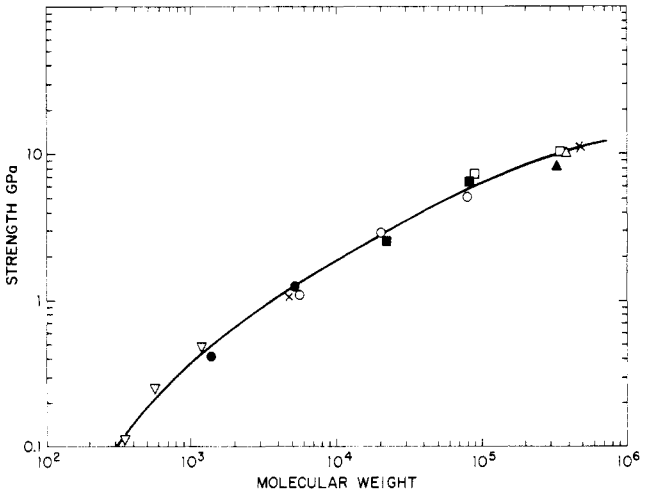

Figure 6. Dependence of the strength (maxima of the curves in Figure 3) on the molecular weight for monodisperse polyethylene fibers. The symbols are for different values for the number m of methyl groups per node. (▽) $m = 5$; (●) $m = 25$; (○) $m = 100$; (×) $m = 200$; (■) $m = 400$; (△) $m = 800$; (□) $m = 1600$; (▲) $m = 3200$. In order to speed up the calculations for the case $m = 5$, we took $\tau = 10^4$.

is clearly due to the molecular weight dependence of the modulus at very low M ($<10^4$) and, at higher M, to the nature of the failure process, which gradually changes from slippage to chain fracture.

5. Discussion

The present kinetic model for fracture of perfectly ordered and fully extended polyethylene chains has revealed the following results: (1) at very low molecular weights, the initial axial modulus depends on the chain length; (2) at $M > 10^4$, the modulus is virtually constant; (3) failure proceeds through slippage at low molecular weights ($M < 8 \times 10^4$); (4) chain fracture occurs at $M > 8 \times 10^4$; (5) at $M > 3 \times 10^5$, failure predominantly involves chain fracture, whereas for $8 \times 10^4 < M < 3 \times 10^5$, both creep and bond rupture occur; (6) straining at 100%/min results in failure within a few seconds at an elongation of a few percent; (7) the elongation at break varies systematically with molecular weight and ranges from 1 to 5% for $M = 6 \times 10^3$ to 5×10^5; (8) the local stress concentration factor can attain values as high as 10; (9) there is no simple relation between the tenacity and the chain length due to changing modes of failure with molecular weight; (10) in the molecular weight range from 2×10^4 to 10^6, the tenacity varies with M approximately as $\sigma \sim M^{0.4}$ (see Figure 5); and (11) extrapolation of the tensile strength to infinite molecular weight yields a value of about 24 GPa (at 8% strain), which lies within the range of previously reported calculations.[5-7] At this point, it is worth noting that the latter value, obtained with $U = 25$ kcal/mol and $\beta = (1.54\ \text{Å})^3$ for the primary bonds is also recovered with $U = 80$ kcal/mol and $\beta = (2.75\ \text{Å})^3$. However, taking $U = 80$ kcal/mol and $\beta = (1.54\ \text{Å})^3$ leads to an unrealistic[5-7] ultimate tensile strength of ~138 GPa (at 46% strain). We have also performed calculations in which the activation energy barrier U (see eq 1) is decreased by the elastic energy (force constant times square of displacement) stored in the bond. Taking for the C–C bond a force constant equal to K_1A/r with an axial modulus $K_1 = 300$ GPa, a chain cross-section $A = 18\ \text{Å}^2$, and a bond length $r = 1.54$ Å leads to an ultimate tensile strength of around 42 GPa (at 14% strain).

Each and everyone of these theoretical results can be readily substantiated with experimental data on highly oriented polyethylene fibers. It is well-known that low molecular weight polyethylene fibers exhibit creep during tensile loading.[29] Also well established is that the modulus of drawn fibers of medium molecular weight depends primarily on the draw ratio and not sensitively on the chain length.[30] Chain fracture during tensile tests of medium and high molecular weight polyethylene has been observed in electron spin resonance experiments.[31] A host of experimental data indicates that short-term (1–10 s) tensile fracture of highly oriented polyethylene fibers occurs at elongations of a few percent[2-4] and that the strain at break increases with increasing molecular weight.[32,33] Remarkably, the empirical power law ($\sigma \sim M^{0.4}$) correlating the molecular weight with the tenacity of moderately oriented fibers (Young's modulus = 50 GPa), found in an earlier experimental study[33] for $5 \times 10^4 < \bar{M}_w < 3.5 \times 10^6$, is recovered in the present theoretical work, albeit for a perfectly ordered structure. These outstanding qualitative agreements between the model at hand and the related experimental observations, in our view, greatly support its usefulness.

With regard to quantitative predictions, i.e., the actual breaking stress and the molecular weights where the modes of fracture change, caution should be exercised. First of all, as was pointed out in the previous section, the values of the model's parameters are not established with great accuracy. Moreover, a number of assumptions were made in the model, many of them to save computer time and memory. It is nonetheless tempting to compare some experimental values against the "predicted" tenacities. First of all, one should bear in mind that the present theoretical work concerns the maximum tensile strength, that is, the tenacity of a perfectly ordered, flawless structure of monodisperse macromolecules. Experimental results are available only for highly oriented fibers of heterodisperse molecular weight that have moduli lower

than the theoretical values. For example, highly drawn polyethylene fibers nowadays are routinely produced[3,4,8-12] with an axial Young's modulus E of 100–150 GPa, σ = 3–5 GPa, and ϵ = 3–5%. The weight-average molecular weight of the polymers used is typically in the range (1–5) × 10^6. $\bar{M}_n$ is usually not reported but supposedly is of the order of (1–5) × 10^5. More recently, data have been published[9,10] on fibers with the following room temperature properties: E = 200 GPa and σ = 7GPa for $\bar{M}_w$ = 2 × 10^6. Assuming, to a first approximation, that the tenacity varies linearly with the modulus, all of these aforementioned values would correspond at K_1 = 300 GPa to σ = 10 GPa for perfectly ordered and extended polyethylene having a weight-average molecular weight in the million range and $\bar{M}_n$ of the order of 10^5. Inspection of the graph in Figure 5 shows a predicted value of σ = 9 GPa and σ = 13 GPa for, respectively, M = 2.5 × 10^5 and M = 10^6 (monodisperse). Previous extrapolations[11] of the tenacity of oriented fibers to a modulus of 300 GPa resulted in a value σ = 8.5 GPa for $\bar{M}_w$ = 1.5 × 10^6 and $\bar{M}_n$ = 2 × 10^5. The admittedly fortuitous, agreement between extrapolated tenacities of experimental fibers and the present calculations provides at least confidence with regard to the choice of the set of values for the model's parameters.

A few comments should be devoted to the size of the "test sample" in the present work. As was mentioned before, the sample typically comprised 6 × 6 × 16 chains. In comparison with the dimensions of experimental fibers, which usually contain (~2 × 10^4) × (2 × 10^4) × (2 × 10^4) chains, our dimensions appear exceptionally small. The obvious question arises how changing the specimen size affects the calculations. After all, it is well-known that fiber length and cross-sectional area have a dramatic effect on its mechanical properties.[34] It was pointed out in the previous section that our system appeared to be homogeneous; i.e., no size effects were observed. The very strong dependence of sample size on the properties of actual fibers originates in the fact that fiber failure is commonly dominated by gross flaws.[34] In the absence of such flaws, as in the present model, indeed no effect is expected.

Finally, the shape of the stress–strain curves after the point of maximum stress (see Figure 3) deserves some discussion. These curves are typified by a rapid, but not sudden, decrease in stress with increasing strain. To our knowledge, such behavior is not commonly observed in tensile tests of high-modulus/high-strength polyethylene. The latter display abrupt, catastrophic failure. The present work indicates that failure of high molecular weight specimens is accompanied by substantial chain fracture, which reduces the chain length (see also Figure 4) to levels where chain slippage occurs. The calculated shape of the stress–strain curves is thus a logical and plausible consequence of the various modes of failure. One possible reason for the absence of such "tails" on the stress–strain curves of actual fibers is the difference in structure between the perfect model fibers and experimental filaments. The latter are known to contain some defects, apart from chain ends, the major one being trapped entanglements. Trapped entanglements provide lateral bonds in the fibers, which will reduce slippage.

In summary, we have presented a kinetic approach to the fracture of a perfectly ordered and oriented polymer fiber. The model is microscopic in nature but is not burdened with the need to provide a detailed structure at the atomic level. Instead, the fiber is represented by an array of nodes joined by oscillating bonds, and bond-breaking events are treated as thermally activated processes. Our approach has been successfully applied to oriented polyethylene filaments and both qualitative and (fortuitious) quantitative agreement between theoretical and related experimental observations has been found. The main disadvantages of our model are that it depends on parameters which may be difficult to measure or calculate for various polymers and that large amounts of computer time are required. For this reason, we believe that the model will probably be of more help in relating the physical characteristics of polymer molecules (molecular weight distribution, orientation, topology, etc.) to their ultimate mechanical properties than in relating chemical structure to them.

Acknowledgment. We thank Dr. A. D. English for a critical reading of the manuscript.

Registry No. Polyethylene (homopolymer), 9002-88-4.

References and Notes

(1) H. H. Kausch, "Polymer Fracture", Springer-Verlag, Berlin, 1978.
(2) See, e.g., "Ultra-High Modulus Polymers", A. Ciferri and I. M. Ward, Eds., Applied Science Publishers, London, 1979.
(3) P. Smith and P. J. Lemstra, *J. Mater. Sci.*, **15**, 505 (1980).
(4) W. Wu and W. B. Black, *Polym. Eng. Sci.*, **19** 1163 (1979).
(5) K. E. Perepelkin, *Angew. Makromol. Chem.*, **22**, 181 (1972).
(6) D. P. Boudreaux, *J. Polym. Sci., Polym. Phys. Ed.*, **11**, 1285 (1973).
(7) B. Crist, M. A. Rafner, A. J. Brower, and J. R. Sabin, *J. Appl. Phys.*, **50**, 6047 (1979).
(8) J. Smook, W. Hammersma, and A. J. Pennings, *J. Mater. Sci.*, **19**, 1359 (1984).
(9) A. V. Savitskii, I. A. Gorshkova, G. N. Shmikk, and I. L. Frolova, *Vysokomol. Soedin., Ser. B*, **25**, 352 (1983).
(10) A. V. Savitskii, I. A. Gorshkova, I. L. Frolova, G. N. Smikk, and A. F. Ioffe, *Polym. Bull.*, **12**, 195 (1984).
(11) P. Smith and P. J. Lemstra, *J. Polym. Sci., Polym. Phys. Ed.*, **19**, 1007 (1981).
(12) T. Ohta, *Polym. Eng. Sci.*, **23**, 697 (1983).
(13) P. J. Flory, *J. Am. Chem. Soc.*, **67**, 2048 (1945).
(14) A. A. Griffith, *Philos. Trans. R. Soc. London*, **221**, 163 (1921).
(15) S. N. Zhurkov and T. P. Sanhirova, *Dokl. Akad, Nauk SSSR*, **101**, 237 (1955).
(16) F. Bueche, *J. Appl. Phys.*, **26**, 1133 (1955); **28**, 784 (1957); **29**, 1231 (1958).
(17) A. Tobolsky and H. Eyring, *J. Chem. Phys.*, **11**, 125 (1943).
(18) J. R. Schaefgen, T. I. Bair, J. W. Ballou, S. L. Kwolek, P. W. Morgan, M. Panar, and J. Zimmerman, in ref 2, p 199.
(19) Reference 1, Chapter 3.
(20) H. H. Kausch and C. C. Hsiao, *J. Appl. Phys.*, **39**, 4915 (1968).
(21) A. V. Dobrodumov and A. M. El'yashevitch, *Sov. Phys.—Solid State (Engl. Transl.)*, **15**, 1259 (1973).
(22) S. N. Zhurkov, V. I. Vettegren, V. E. Korsukov, and I. I. Novak, "Proceedings of the 2nd International Conference on Fracture", Brighton, Chapman and Hall Ltd. London, 1969, p 545. S. N. Zhurkov and V. E. Korsukov, *J. Polym. Sci., Polym. Phys. Ed.*, **12**, 385 (1974); *Sov. Phys.—Solid State (Engl. Transl.)*, **15**, 1379 (1974).
(23) We chose δy = 0.1%, which, for a typical node made of 100 methyl groups (see section 4), corresponds to a shear strain of around 10% for a single van der Waals bond. That latter value compares favorably with the 5% thermal amplitude of the van der Waals bond in polyethylene (see H. H. Kausch and J. Becht, in "Deformation and Fracture of High Polymers", H. H. Kausch et al., Eds., Plenum Press, New York, 1973, 317). As far as we could determine, a decrease of δy by a factor of 10 does not significantly affect our results for the maximum strength. We have also performed calculations in which the secondary bonds are re-formed at a rate given by eq 1, with σ_i = 0. These two alternative procedures for the reformation of the secondary bonds lead, within experimental error, to similar results for the maximum strength.
(24) E. H. Andrews and P. E. Reed, *Adv. Polym. Sci.*, **27**, 1 (1978).
(25) D. N. de G. Allen, *Relaxation Methods*, Mc Graw Hill, N. Y (1954).
(26) I. M. Ward, "Mechanical Properties of Solid Polymers", 2nd ed., Wiley, New York, 1983, p 270.
(27) Such a low value for the activation energy is also confirmed by thermal degradation experiments, which are seen to proceed in two stages: one characterized by a low activation energy (25–30 kcal/mol) and the other by a higher value (50–60 kcal/mol). See V. R. Regel, A. V. Amelin, O. F. Pozdnyakov,

T. P. Sanfirova, and A. F. Ioffe, Preprint of the International Symposium on Macromolecules, Helsinki, Finland, Jul 2-7, 1972, Vol. 5, 163.
(28) In that new representation, the stochastic process still visits primary bonds with the same probability as secondary bonds, since one must not overlook the fact that each node itself actually represents m primary bonds aligned in series along the y axis.
(29) D. L. M. Cansfield, I. M. Ward, D. W. Woods, A. Buckley, J. M. Pierce, and J. L. Wesley, *Polym. Commun.*, **24**, 130 (1983).
(30) G. Capaccio, A. G. Gibson, and I. M. Ward, ref 2, p 12.
(31) See ref 1, Chapter 7.
(32) W. G. Perkins, N. J. Capiati, and R. S. Porter, *Polym. Sci. Eng.*, **16**, 200 (1976).
(33) P. Smith, P. J. Lemstra, and J. P. L. Pijpers, *J. Polym. Sci., Polym. Phys. Ed.*, **20**, 2229 (1982).
(34) A. Kelly, "Strong Solids", 2nd ed., Clarendon Press, Oxford, 1973, Chapter 2.

Adsorption of Polyacrylamide on Solid Surfaces. Kinetics of the Establishment of Adsorption Equilibrium

E. Pefferkorn, A. Carroy, and R. Varoqui*

Centre de Recherches sur les Macromolécules (CNRS), 67083 Strasbourg Cedex, France.
Received March 13, 1985

ABSTRACT: The kinetics of the establishment of adsorption equilibria of polyacrylamide onto chemically modified glass beads was studied by a radioactive tracer method using ^{3}H-labeled polymers. The adsorption rates were determined as a function of temperature and surface affinity by varying the surface density of the interacting sites. The experimental conditions were chosen to minimize diffusion effects. Quantitative analysis shows that adsorption is governed by the structure of the surface layer; in particular, the adsorption rate is proportional to the number of free interacting surface sites. The role of the diffuse polymer layer as a barrier rate-limiting factor is also discussed.

Introduction

In previous work we measured the rate of exchange of adsorbed ^{3}H-labeled polymers with nonlabeled polymers in the bulk and analyzed the adsorption rates in the region of adsorption equilibrium.[1] In this paper, we discuss the factors involved in the establishment of adsorption equilibrium.

A study of the rate of establishment of adsorption equilibrium of polymers at solid/liquid interfaces is of fundamental importance in many areas (polymer processing, flocculation of colloidal particles, adhesion, coating, etc.) From a conceptual point of view, the adsorption of polymers implies rate-controlling factors that are not encountered with ordinary molecules. In particular, because of their chainlike structure, the adsorbed surface films of polymers are structurally similar to the surface of a gel, and the rate of adsorption depends not only on the mechanism of adherence to the surface by multiple points of physical adsorption but also on the rate of penetration of a gellike layer. Adsorption rates of polymers have been studied in the past.[2] However, the most interesting features were often blurred by trivial ones (for example, mass transfer by diffusion of polymers to the surface, which depends heavily on the hydrodynamic conditions, presents no interest on its own). Furthermore, the experimental conditions were frequently such that equilibrium was rapidly established in a few minutes or even a few seconds[3,4] and, owing to experimental difficulties, the kinetic parameters could not be assessed with certainty.

In this study of the adsorption of polyacrylamide in aqueous solution on the surface of modified silica particles, the experimental conditions were chosen to ensure a certain number of meaningful points: (i) the nature and density of the surface sites interacting with the polymer were characterized quantitatively, and one objective was to correlate the adsorption kinetics with the "active" site density; (ii) experimental conditions were chosen to minimize bulk diffusion effects (very often, adsorption was carried out in a semiinfinite and unstirred medium by transferring adsorbent plates into a vessel containing the polymer solution); (iii) a very sensitive determination of adsorption was obtained via ^{3}H labeling.

Table I
Characteristics of Glass Beads

sample code	mean diam, μm	spec surface area, $cm^2 \cdot g^{-1}$	% comp [AlOH]/[SiOH]
AS0	34	780	0
AS1	34	780	5
AS2	34	780	12

Experimental Section

1. Polymer. Radioactive polyacrylamide was prepared by radical polymerization in the presence of traces of acrolein. After fractionation, the resulting material was reacted in aqueous solution with tritiated potassium borohydride to yield the following chemical structure (details are given in ref 1):

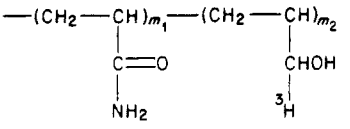

$m_1/m_2 = 10^3$

The characteristics of the sample used in this study are as follows: $M_w = 1.2 \times 10^6$; polydispersity (GPC) = 1.25; specific radioactivity = 1.12×10^8 counts·min^{-1}·g^{-1}.

2. Adsorbents. Nonporous glass beads (Verre et Industrie) of 34-μm average diameter were used as the adsorbent. The surface was first made hydrophilic by soaking for 24 h in hot hydrochloric acid medium

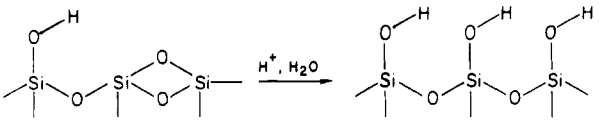

and was then treated with aluminum chloride in chloroform in order to replace some silanols (SiOH) by aluminum chloride

0024-9297/85/2218-2252$01.50/0